Simplification of the resonance fluorescence spectrum by detuning from absorption features

ARTICLE *in* THE JOURNAL OF PHYSICAL CHEMISTRY · DECEMBER 1984

Impact Factor: 2.78 · DOI: 10.1021/j150669a037

3 AUTHORS, INCLUDING:

Mario Blanco
King Abdullah University of Science and Tech…
64 PUBLICATIONS **1,721** CITATIONS

SEE PROFILE

expected to be smaller. Namely, within the ΔN coefficient a large $|\mu^0|$ (of hard atom) is then multiplied by a small hardness $|\eta|$ of the partner, and vice versa. This should lead to a better cancellation of terms. The same is true for the ΔZ coefficients, since there large $|\mu^0|$ (of hard atom) is multiplied by a small coupling derivative α (of soft atom), and vice versa. Again, the best predictions from the Sanderson principle are expected in the *soft-soft* case for which both the ΔN and ΔZ coefficients should reach the minimum values.

We therefore conclude that the Sanderson principle is expected to exhibit increasing deviations as the hardness parameters of the constituent atoms increase. A more detail analysis of this qualitative observation is given elsewhere.[20]

(20) R. F. Nalewajski, *J. Phys. Chem.*, submitted.

Finally, we would like to observe that the coupling derivative α_X represents the *global*, atomic analogue of the *local*, molecular frontier (or Fukui) function of Parr and Yang,[21] which rationalizes the frontier-electron theory of chemical reactivity.[22]

Acknowledgment. We thank Professor Libero J. Bartolotti for providing us with the Hartree-Fock data. R.F.N. thanks also Professor Robert E. Wyatt for his generous hospitality in Austin, where this manuscript was prepared. This work was supported in part by a research grant from the National Science Foundation and a grant from the Institute of Low Temperatures and Structural Research, Polish Academy of Sciences, Wrocław, Poland.

(21) R. G. Parr and W. Yang, *J. Am. Chem. Soc.*, **106**, 4049 (1984).
(22) K. Fukui, "Theory of Orientation and Stereoselection", Springer-Verlag, West Berlin, 1973.

Simplification of the Resonance Fluorescence Spectrum by Detuning from Absorption Features

David J. Tannor,*† Mario Blanco,‡ and Eric J. Heller†§

T-12 Group, Los Alamos National Laboratories, Los Alamos, New Mexico 87545, and the Department of Chemistry, University of California, Los Angeles, California 90024 *(Received: July 16, 1984)*

We propose detuning the incident laser from any of the stationary vibrational features identified by the Smalley group (e.g., $6b_0^1$) in the long-tail alkylbenzenes. We suggest that, in a relative sense, relaxed fluorescence lines will disappear and resonance fluorescence lines will grow back as the detuning frequency is increased. Our claim is based on the time-energy uncertainty principle, $\Delta\omega\,\tau \simeq 1$. By detuning, $\Delta\omega$ increases, τ goes down, and the zeroth-order vibrational state has less and less time to evolve into the tail.

Introduction

The recent experiments of the Smalley group on the alkylbenzenes[1] have attracted considerable attention.[2,3] These experiments combine the latest techniques for studying state-to-state chemistry—a high-resolution laser and a supersonic jet—with an ideally selected molecule. The alkylbenzenes have a well-defined chromophore, the benzene ring, and an electronically inactive segment, the alkyl tail. The Smalley group varied the length of the alkyl tail from one to seven methyl groups and monitored the absorption spectrum. The absorption spectrum looks qualitatively the same for the set of alkylbenzenes; in particular three vibrational features, labeled 6b, 12, and 18a, hardly changed their position as a function of tail length (see Figure 1a-c). This was taken as an indication that the normal modes of vibration corresponding to each of these vibrational features is localized to the ring atoms (see Figure 1d). These "zeroth-order" states seem to be ideally suited for depositing energy in one part of a large molecule and having it stay there, violating the statistical assumptions of RRKM theory and giving credence to laser selective chemistry ideas.

The Smalley group tuned their incident laser to one of these stationary vibrational features—for definiteness, say, the $6b_0^1$ feature—and monitored the dispersed fluorescence spectrum (DFS). They saw dramatic changes in the DFS spectrum with tail length, including the disappearance of "resonance" fluorescence lines, the growth of "relaxed" fluorescence lines, and a narrowing up of the relaxed fluorescence with the longer tail species. These three trends were explained as the signature of intramolecular vibrational energy transfer (IVR) from ring to tail on a time scale shorter than the fluorescence lifetime. Figure 1e shows the DFS for three members in the sequence of molecules.

In this article we propose detuning the incident laser light from the zeroth-order vibrational feature in the long-tail alkylbenzenes. We find the use of the term "resonance" fluorescence for a subset of lines in the DFS confusing. We prefer the term "tense" fluorescence. We suggest that, in a relative sense, relaxed fluorescence lines will disappear and tense fluorescence lines will grow back, as the detuning frequency is increased. The broad bands of relaxed fluorescence lines (shown most clearly in the expanded trace in Figure 1f) should disappear as the detuning is increased, the reverse of the trend originally illustrated in Figure 1e. The DFS of hexylbenzene should resemble that of shorter and shorter tail alkylbenzenes, until resembling the spectrum of benzene itself as the detuning is increased!

Our claim is based on the time-energy uncertainty principle, $\Delta\omega\,\tau \simeq 1$. Tuning directly to the $6b_0^1$ feature implies $\Delta\omega \to 0$, $\tau \to \infty$. The $6b_0^1$ zeroth-order feature has essentially infinite time to evolve from the ring to the tail. The resulting DFS is full of relaxed fluorescence lines. By detuning, $\Delta\omega$ increases, τ goes down, and the zeroth-order state has less and less time to evolve into the tail. The resulting DFS shows a smaller and smaller fraction of relaxed fluorescence lines. Our principal numerical studies will be ratios of tense fluorescence (TF) to total dispersed fluorescence

* Address correspondence to this author at the James Franck Institute, University of Chicago, Chicago, IL 60637.
† Los Alamos National Laboratories.
‡ University of California.
§ Present address: Department of Chemistry, University of Washington, Seattle, WA.

(1) (a) Hopkins, J. B.; Powers, D. E.; Smalley, R. E. *J. Chem. Phys.* **1980**, *72*, 5039. (b) Hopkins, J. B; Powers, D. E.; Mukamel, S.; Smalley, R. E. *J. Chem. Phys.* **1980**, *72*, 5049. (c) Hopkins, J. B.; Powers, D. E.; Smalley, R. E. *J. Chem. Phys.* **1980**, *73*, 683.
(2) Freed, K. F.; Nitzan, A. *J. Chem. Phys.* **1980**, *73*, 4765.
(3) Mukamel, S.; Smalley, R. E. *J. Chem. Phys.* **1980**, *73*, 4156.

0022-3654/84/2088-6240$01.50/0

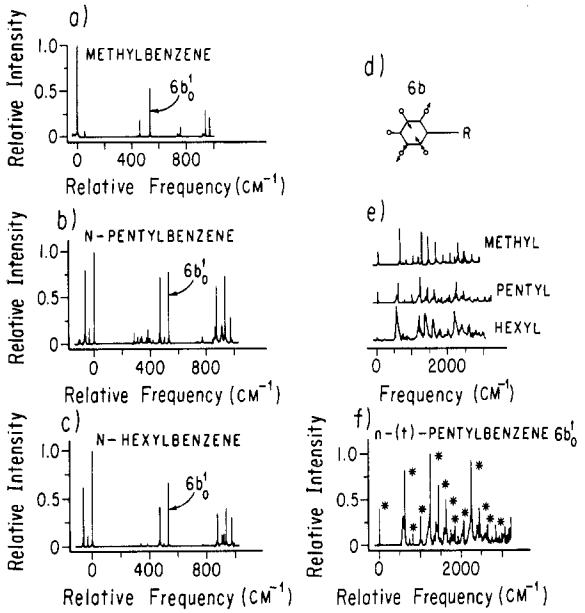

Figure 1. (a) Absorption spectrum for jet-cooled methylbenzene. Courtesy of R. E. Smalley. The arrow indicates the $6b_0^1$ vibrational feature. The inset shows the form of the 6b normal mode. (b) Same as part a but for pentylbenzene. (c) Same as part a but for hexylbenzene. (d) Dispersed fluorescence spectrum of jet-cooled methylbenzene, pentylbenzene, and hexylbenzene. The incident light was tuned to the $6b_0^1$ vibrational feature. Courtesy of R. E. Smalley. (e) Expanded trace of DFS for jet-cooled pentylbenzene. Asterisks indicate "tense" fluorescence lines. Broad features represent relaxed fluorescence.

(TDF) as a function of incident frequency. We expect the ratio to dip on resonance with the vibrational feature and go to 1 as $\Delta\omega$ increases.

Theory

The theory of resonance fluorescence, as it applies to the alkylbenzene experiments, is formally identical with the theory of resonance Raman scattering (RRS). We take as our starting point some time-dependent formulas with their wave packet interpretation, originally developed for RRS.[4,5]

The amplitude for RRS from initial state χ_i to final state χ_f is given by

$$\alpha_{fi}(\omega_I) = \int_0^\infty \langle\phi_f|\phi_i(t)\rangle e^{i(\omega_i+\omega_I)t-\Gamma t}\,dt \tag{1}$$

where

$$|\phi_i\rangle = \mu|\chi_i\rangle$$

$$|\phi_f\rangle = \mu|\chi_f\rangle$$

$$|\phi_i(t)\rangle = e^{-iHt/\hbar}|\phi_i\rangle \tag{2}$$

ω_i is the ground-state energy of χ_i, ω_I is the incident laser frequency, and Γ is the radiative lifetime. H is the excited Born–Oppenheimer (BO) Hamiltonian. The intensity of a peak in the jet-cooled DFS is given by

$$I^f(\omega_I) = k\omega_I\omega_S^3|\alpha_f(\omega_I)|^2 \tag{3}$$

where k is a constant, ω_S is the frequency of scattered radiation, and the initial state i is here and henceforth assumed equal to 0.

The intensity for Rayleigh scattering will play an important role in this article:

$$\alpha_0(\omega_I) = \int_0^\infty \langle\phi_i|\phi_i(t)\rangle e^{i(\omega_i+\omega_I)t-\Gamma t}\,dt \tag{4a}$$

$$I^0(\omega_I) \propto |\alpha_0(\omega_I)|^2 \tag{4b}$$

Equation 1 is amenable to a wave packet interpretation. ϕ_i is an initial wave packet prepared on the excited BO surface. It is a nonstationary state and propagates on the excited surface, in general leaving the Franck–Condon region. The time-dependent wave packet is overlapped with the final state of interest, ϕ_f, and the half-Fourier transform is performed to obtain the RRS amplitude.

An alternative interpretation of eq 1 was offered in ref 5. We define the Raman wave function (RWF), $R(\omega_I)$, as

$$R(\omega_I) = \int_0^\infty \phi_i(t)e^{i(\omega_i+\omega_I)t-\Gamma t}\,dt \tag{5}$$

$$\sim \sum_n \phi_i(t_n)e^{i(\omega_i+\omega_I)t-\Gamma t_n} \tag{6}$$

The Raman wave function may be viewed as a superposition of wave packets at different times, $\phi_i(t_n)$, added together with a phase factor given by $e^{i(\omega_i+\omega_I)t_n}$. The RWF is sensitive to the experimentally controllable parameter ω_I: if $\omega_i + \omega_I$ is resonant with the excited BO surface, the wave packets add constructively and an extended wave function is produced. If $\omega_i + \omega_I$ is nonresonant or preresonant, the wave packets destroy each other after a time, Δt, equal to the reciprocal of the frequency mismatch. The resulting wave function is localized to the FC region. Indeed, this picture of a Raman wave function is closely related to a dynamical formula for a quantum eigenfunction.[6]

The RRS amplitude is now given by

$$\alpha_f = \langle\phi_f|R(\omega_I)\rangle \tag{7}$$

the overlap of the RWF with the final state of interest. In addition, the total dispersed fluorescence, I_{TDF}, is given by the self-overlap of R

$$I_{TDF}(\omega_I) = \sum_f I^f(\omega_I) = \langle R(\omega_I)|R(\omega_I)\rangle \tag{8}$$

In eq 8 and the remainder of this letter we assume the Condon approximation (constant μ) and we neglect the frequency-dependent prefactors in eq 3. These factors are easily reintroduced.

The application of the above formalism to the interpretation of the Smalley group experiments requires a significant restructuring. By virtue of the well-defined vibrational structure in Figure 1a there is significant additional information about dynamics on the excited BO surface above and beyond that implied by the initial state ϕ_i. Tuning on or near a vibrational feature selects for a particular zeroth-order state. We begin by expanding ϕ_i in terms of zeroth-order states, l_i^n:

$$\phi_i = \sum_n c_n l_i^n \tag{9}$$

Then

$$R(\omega_I) = \int_0^\infty e^{-iHt/\hbar}\phi_i e^{i(\omega_i+\omega_I)t-\Gamma t}\,dt \tag{10a}$$

$$= \sum_n c_n \int_0^\infty e^{-iHt/\hbar} l_i^n e^{i(\omega_{n'}+\gamma\omega)t}e^{-\Gamma t}\,dt \tag{10b}$$

$$\approx c_{n'}\int_0^\infty e^{-iHt/\hbar} l_i^{n'} e^{i(\omega_{n'}+\gamma\lambda)t}e^{-\Gamma t}\,dt \tag{10c}$$

Furthermore, we are interested in the summed intensity in the

(4) Lee, S.-Y.; Heller, E. J. *J. Chem. Phys.* **1979**, *71*, 4777.

(5) Heller, E. J.; Sundberg, R. L.; Tannor, D. J. *J. Phys. Chem.* **1982**, *86*, 1822.

(6) A quantum eigenfunction may be written

$$\psi_E = \lim_{T\to\infty} \frac{1}{T}\int_{-T}^{T}\phi_i(t)e^{iEt/\hbar}\,dt$$

$$\sim \sum_n e^{-iHt_n/\hbar}\phi_i e^{iEt_n/\hbar}$$

See, for example: DeLeon, N.; Davis, M. J.; Heller, E. J. *J. Chem. Phys.* **1984**, *80*, 794.

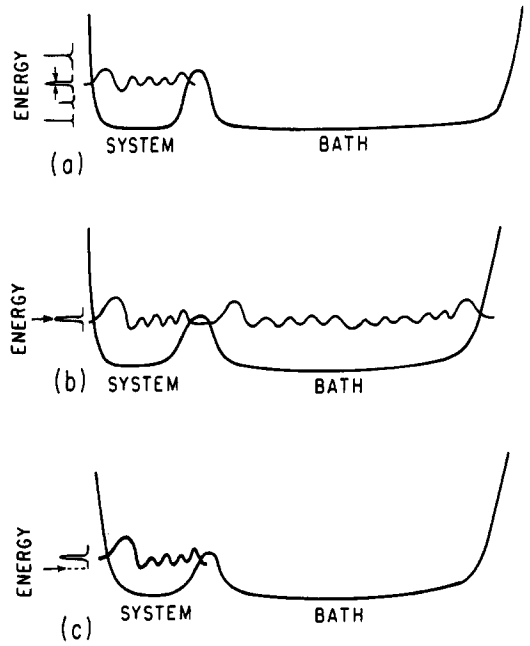

Figure 2. (a) Schematic zeroth-order vibrational feature (indicated by arrows) and corresponding zeroth-order state for a system with a large bath. (b) Schematic Raman wave function for the same potential as in part a, for $\omega_l + \omega_I$ tuned directly to the zeroth-order vibrational feature. (c) Schematic Raman wave function for the same potential as in part a, but $\omega_l + \omega_I$ is detuned from the vibrational feature.

tense fluorescence (TF) lines, $S(\omega_I)$, not really the intensity in a single TF line:

$$S(\omega_I) = \sum_{f'} I^{f'}(\omega_I) \tag{11}$$

where f' is an index running over TF lines. Now

$$\phi_{f'} = \sum_n c_n^{f'} l_i^n \tag{12}$$

so

$$S(\omega_I) = \sum_{f'} |\langle \phi_{f'} | R(\omega_I)\rangle|^2 \tag{13a}$$

$$\sim \sum_{f'} |c_n^{f'}|^2 |\langle l_i^{n'} | R(\omega_I)\rangle|^2 \tag{13b}$$

$$= |\langle l_i^{n'} | R(\omega_I)\rangle|^2 \tag{13c}$$

There are two physical assumptions involved in the derivation of eq 10c and 13c: (1) The small set of $\{l_i^n\}$ states are complete with respect to the expansion of ϕ_i as well as all the $\phi_{f'}$ states. This assumption was used in eq 9 and 12. The sparse nature of the zeroth-order absorption spectrum of hexylbenzene suggests just such an expansion of ϕ_i. The assumption is reasonable for the $\phi_{f'}$ states as well, since they are constrained, by definition, to have zero quanta in all bath modes. (2) All of the dynamics is governed by a single zeroth-order state, $l_n^{n'}$, in the expansion of ϕ_i. The particular zeroth-order state is determined by the vibrational feature to which the incident light is tuned ($\omega_i + \omega_I = \omega_{n'} + \Delta\omega$). This assumption accounts for the neglect of the sum over n in arriving at eq 10c and 13b and is valid if other vibrational features are well separated in energy. Henceforth, we will omit the superscript n'.

Taking together eq 8 and 13c, the fraction of $I_{TDF}(\omega_I)$ which $S(\omega_I)$ represents is given by

$$\frac{S(\omega_I)}{I_{TDF}(\omega_I)} = \frac{|\langle l_i | R(\omega_I)\rangle|^2}{\langle R(\omega_I) | R(\omega_I)\rangle} \tag{14}$$

We note that eq 14 has the form of a probability, with a maximum allowed value of 1. This expression reflects the following intuitive idea: l_i is a zeroth-order state whose nodes lie along the system coordinate (Figure 2a). This normalized state serves as a *probe* of the fraction of the RWF which builds up in the system coordinate. If one tunes ω_I directly to a vibrational absorption feature, the resulting RWF is extended over system and bath coordinates (Figure 2b). The fractional overlap with l_i is small. If one detunes ω_I from the vibrational absorption feature, one prepares a RWF which reflects just the early time dynamics, i.e., motion in the system coordinate (see Figure 2c). The fractional overlap with l_i is close to 1. The denominator in eq 14 normalizes the overlap: $\langle R|R\rangle$ will be large for ω_I on resonance (recall that R is not a normalized wave function) and small for ω_I detuned.

Equation 14 is noteworthy in that it formulates the ratio of S to I_{TDF} without any reference to the final states, $\phi_{f'}$. The spectral features in the DFS associated with S are usually disparate and unevenly spaced. By grouping these spectral intensities together we free ourselves from the whims and vagaries of the *ground* BO surface. The dynamics on the *excited* BO surface exclusively is revealed.

It is instructive to rewrite eq 14 in another way:

$$\langle R|R\rangle = \int_0^\infty \left\langle l_i(t') | e^{-i(\omega_l+\omega_I)t'} e^{-\Gamma t'}\, dt' \int_0^\infty |l_i(t)\right\rangle e^{i(\omega_l+\omega_I)t} e^{-\Gamma t}\, dt \tag{15}$$

Following a derivation in ref 5 we define

$$u = t + t'$$
$$v = t - t'$$

We obtain

$$\langle R|R\rangle = \tfrac{1}{2}\int_{-\infty}^{\infty} \langle l_i | e^{-iHv/\hbar} | l_i\rangle e^{i(\omega_l+\omega_I)v}\, dv \int_{|v|}^{\infty} e^{-\Gamma u}\, du \tag{16a}$$

$$= (1/2\Gamma) \int_{-\infty}^{\infty} \langle l_i | l_i(t)\rangle e^{i(\omega_l+\omega_I)t} e^{-\Gamma|t|}\, dt \tag{16b}$$

Substituting this expression in the denominator of eq 14 and the definition of $R(\omega_I)$ in the numerator yields the following intriguing expression:

$$\frac{S(\omega_I)}{I_{TDF}(\omega_I)} = \frac{\left|\int_0^\infty \langle l_i | l_i(t)\rangle e^{i(\omega_l+\omega_I)t} e^{-\Gamma t}\, dt\right|^2}{(1/2\Gamma)\int_{-\infty}^{\infty} \langle l_i | l_i(t)\rangle e^{i(\omega_l+\omega_I)t} e^{-\Gamma t}\, dt} \tag{17}$$

There are two points to notice immediately about eq 17. (1) The expression depends only on $\langle l_i | l_i(t)\rangle$. The absorption spectrum is given by

$$\sigma_{ABS}(\omega_I) = k\omega_I \int_{-\infty}^{\infty} \langle l_i | l_i(t)\rangle e^{i(\omega_l+\omega_I)t}\, dt \tag{18}$$

where k is some constant. Hence, $\langle l_i | l_i(t)\rangle$ is available experimentally via Fourier transform and eq 17 may be calculated by independent means. (2) The expression in the numerator for S bears a close resemblance to eq 4a for Rayleigh scattering. The sum of the intensity in the TF peaks is the analogue on a picosecond time scale of the intensity in the Rayleigh peak on a femtosecond time scale. Each of these intensities, relative to the TDF, reflects the proportion of short-time dynamics in the DFS: the probability of fluorescing from the system coordinate in the case of S, the probability of fluorescing from the initial phase space cell in the case of Rayleigh scattering.

It is worth mentioning several explicit results which stem from eq 17. (1) In $\langle l_i | l_i(t)\rangle$ limit $\Delta\omega \to \infty$, $\tau \to 0$. We expand $\langle l_i | l_i(t)\rangle$ in a Taylor series about $t = 0$ and keep just the first term:

$$\langle l_i | l_i(t)\rangle = 1 + \ldots \tag{19}$$

The ratio, eq 17, becomes

$$\frac{\lim_{\Delta\omega\to\infty} S(\Delta\omega)}{\lim_{\Delta\omega\to\infty} I_{TDF}(\Delta\omega)} = \frac{\left|\int_0^\infty e^{i\Delta\omega t} e^{-\Gamma t}\, dt\right|^2}{(1/2\Gamma)\int_{-\infty}^{\infty} e^{i\Delta\omega t} e^{-\Gamma|t|}\, dt} = 1 \tag{20}$$

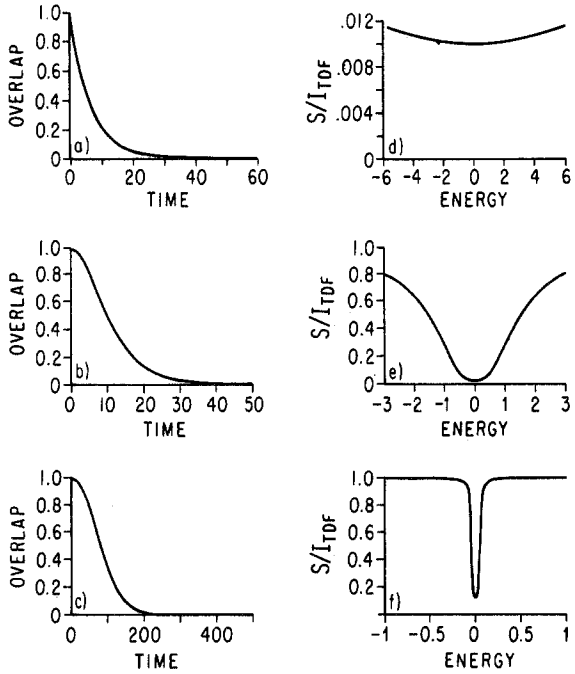

Figure 3. (a) $C(t) = e^{(-\Delta^2/\gamma^2)(\gamma t - 1 + e^{-\gamma t})}$, $\Delta = 0.15$, $\gamma = 15$, $\Gamma = 0.0015$. (b) Same as part a but $\Delta = 0.15$, $\gamma = 0.15$. (c) Same as part a but $\Delta = 0.015$, $\gamma = 0.0015$. (d) $S(\omega)/I_{TDF}(\omega)$ for the parameters given in part a. (e) $S(\omega)/I_{TDF}(\omega)$ for the parameters given in part b. (f) $S(\omega)/I_{TDF}(\omega)$ for the parameters given in part c.

In the limit of short-time dynamics all fluorescence is tense fluorescence!

(2) At $\Delta\omega = 0$ eq 17 becomes

$$\frac{S(0)}{I_{TDF}(0)} = \frac{|\int_0^\infty \langle I_i|I_i(t)\rangle e^{-\Gamma t}\,dt|^2}{(1/2\Gamma)\int_{-\infty}^{\infty}\langle I_i|I_i(t)\rangle e^{-\Gamma|t|}} \tag{21}$$

Assuming for the moment that $\langle I_i|I_i(t)\rangle$ is real, we find the ratio can be written as

$$\frac{\int_0^\infty \langle I_i|I_i(t)\rangle e^{-\Gamma t}\,dt}{\int_0^\infty e^{-\Gamma t}\,dt} \tag{22}$$

We have written the integral $[0,\infty]$ for $^1/_2[-\infty,\infty]$ and $\int_0^\infty e^{-\Gamma t}\,dt = 1/\Gamma$. Since $\Delta\omega = 0$ corresponds to the minimum of the ratio, eq 22 has the interpretation that the ratio at its minimum is the integrated area of the correlation function divided by the integrated area until Γ cuts off the dynamics (see Figure 3). For $|\Delta\omega| > 0$, the dynamics is effectively shorter than the Γ lifetime; the correlation function represents a larger fraction of the effective dynamics and the ratio rises. For general, complex $\langle I_i|I_i(t)\rangle$ the ratio has an upper bound of twice the above value.

(3) Assume that

$$\langle I_i|I_i(t)\rangle = e^{-\alpha|t|} \tag{23}$$

This is a form often deduced from picosecond and other explicitly time-domain experiments;[7] it is also derived from the Bixon–Jortner step ladder model for IVR.[8] In this case the ratio is

$$\frac{S(\Delta\omega)}{I_{TDF}(\Delta\omega)} = \frac{|\int_0^\infty e^{-\alpha t}e^{i\Delta\omega t}e^{-\Gamma t}\,dt|^2}{(1/2\Gamma)\int_{-\infty}^{\infty}e^{-\alpha|t|}e^{i\omega t}e^{-\Gamma|t|}\,dt} = \frac{\Gamma}{\Gamma+\alpha} \tag{24}$$

The result is independent of ω_i! For a correlation function that rigorously decays exponentially, the line shape of the zeroth-order vibrational feature is rigorously Lorentzian, and the effect we have been describing is absent. An essential point here is that the decay cannot be rigorously exponential. The autocorrelation function, $C(t) = \langle I_i|I_i(t)\rangle$, must be rounded at $t = 0$ ($dC/dt = 0$); equivalently, the line shape must decay to zero in the wings somewhat faster than Lorentzian for any physical system. We explore below the quantitative relationship between the rounding of the cusp at $t = 0$ and the frequency dependence of the ratio plots.

We model the autocorrelation function with a simple functional form:

$$C(t) = e^{-\Delta^2/\gamma^2(\gamma|t|-1+e^{-\gamma|t|})} \tag{25}$$

This form was derived by Kubo for a quantum level coupled to a Gaussian distribution of bath states.[9] It has the appealing feature of a Gaussian decay at short times, $e^{-\Delta^2t^2}$, and an exponential decay at long times, $e^{-\Delta^2|t|/\gamma}$. This satisfies the physical requirement of the roundness at $t = 0$ while allowing for a decay as exponential as desired by adjusting Δ and γ. Figure 3a–c shows $C(t)$ for a range of Δ and γ, ranging from exponential to Gaussian. The values of Δ and γ are 1.5 and 15, 0.15 and 0.15, and 0.015 and 0.0015, respectively, and $\Gamma = 0.0015$. Figure 3d–f shows $S(\Delta\omega)/I_{TDF}(\Delta\omega)$. Note that while the deviation from exponential in Figure 3a is microscopic, the ratio plot in Figure 3d still bears the imprint of the roundness at $t = 0$. Figure 3e,f, for more Gaussian-like line shapes, shows the resonant dip more dramatically.

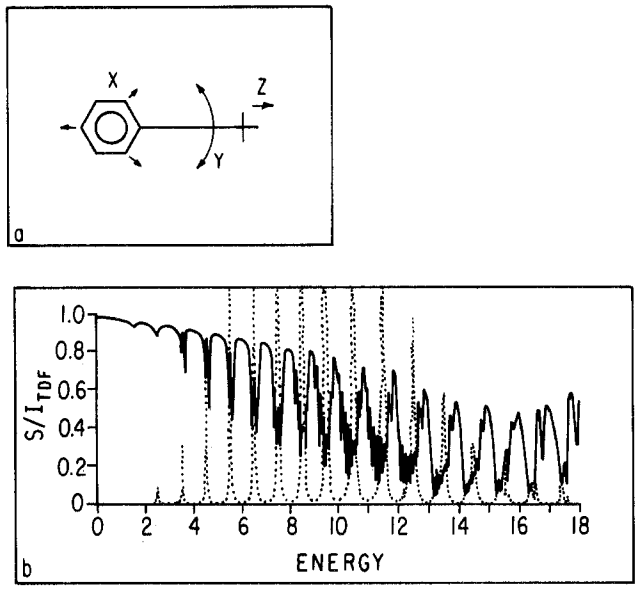

Figure 4. (a) Form of the normal mode coordinates x, y, and z for 3-d anharmonic system discussed in the text. (b) $S(\omega)/I_{TDF}(\omega)$ for 3-d anharmonic system. Parameters given in text. Dashed line is the absorption spectrum.

3-d Model System

We have examined a 3-d, anharmonic, Fermi resonant quantum-mechanical system. The excited-state Hamiltonian, H_{ex} is

$$H_{ex} = T + \tfrac{1}{2}\omega_x^2(x-x_0)^2 + \tfrac{1}{2}\omega_y^2 + \tfrac{1}{2}\omega_z^2(z-z_0)^2 + \lambda(x-x_0)y^2 + \lambda y^2(z-z_0) \tag{26}$$

The ground-state Hamiltonian, H_g, is

$$H_g = T + \tfrac{1}{2}\omega_x^2 + \tfrac{1}{2}\omega_y y^2 + \tfrac{1}{2}\omega_z z^2 \tag{27}$$

$$x_0 = 4 \qquad z_0 = 0.4 \qquad \lambda = -0.11 \qquad \omega_x = \omega_z = 1 \qquad \omega_y = 1.1$$

This system is a crude model for the alkylbenzenes and illustrates one possible mechanism by which energy escapes from the benzene ring. Consider the diagram in Figure 4a. The x coordinate represents a totally symmetric normal mode of vibration localized

(7) This is the form taken in ref 1c, for example.

(8) Bixon, M.; Jortner, J. *J. Chem. Phys.* **1968**, *48*, 715.

(9) Kubo, R. *Adv. Chem. Phys.* **1969**, *15*, 101.

to the benzene ring (e.g., mode 12 in the notation of ref 1). Thus, the x mode may be well displaced on the excited surface, corresponding to a large change in equilibrium geometry. The y mode is an asymmetric motion, for instance, a skeletal bend of the ring plus tail. Symmetry dictates that this mode enter in the Hamiltonian only in even powers (i.e., y^2, xy^2, etc.) and, furthermore, that this mode not be displaced ($y_0 = 0$). The z mode corresponds to a longitudinal tail stretch. Although formally this mode may be displaced on the excited surface, since it is not part of the chromophore it is likely to remain relatively unchanged in H_{ex} (hence $z_0 = 0.4$).

The excited Hamiltonian was diagonalized in a harmonic oscillator basis set, using all states up to energy 21. The tense fluorescence lines are identified with the Rayleigh peak, as well as the fundamental and overtones in mode x. The sum of the TF lines (up to the 31st overtone) was computed as a function of incident light frequency and then divided by the total dispersed fluorescence at that frequency. Figure 4b shows S as a fraction of TDF. Also shown in Figure 4b, in dotted lines, is the absorption spectrum. Note the dips in the ratio of S/TDF on resonance with the absorption features! This then is the signature that energy has flowed out of the initially plucked mode (x), and into the others (y and z). One may think of the dip at each vibrational feature (falling at integer energies) as corresponding to the dip in Figure 3f. The discrepancies with the idealized Figure 3f arise from substructure in the absorption feature (recurrences in the correlation function) as well as from some interference between the different vibrational bands.

Conclusions

In this letter we focused on the ratio of "tense" (unrelaxed) fluorescence intensity to the total dispersed fluorescence intensity as a function of detuning energy. Detuning corresponds to short-time dynamics, not giving the initial state a chance to relax, and hence the relative amount of TF intensity increases. The tense and relaxed fluorescence lines are well characterized in the alkylbenzene experiments of the Smalley group. Detuning from the $6b_0^1$ feature in hexylbenzene, for example, should give rise to an DFS spectrum characteristic of a shorter and shorter tail alkylbenzene until ultimately the DFS spectrum of benzene should be recovered.

One might imagine analogous behavior for radiationless processes in large molecules. For instance, if there is an intersystem crossing, and the molecule phosphoresces, by detuning from the zeroth-order (singlet) vibrational feature one should be able to reduce the fraction of phosphorescence in the total luminescence. By the same token, the technique may have direct bearing on laser selective chemistry. Imagine substituting an iodine for a hydrogen near the ring and a bromine for a hydrogen way out on the tail. Further, suppose tuning on resonance would photofragment both the iodine and bromine atoms. By detuning, however, one should be able to dissociate the iodine without dissociating the bromine.

In this paper we have just scratched the surface of the detuning idea. We examined just the ratio of I_{TF}/I_{TDF}. In fact, there is a tremendous amount of information in the relaxed fluorescence lines, and their intensity as a function of frequency. If these lines are properly assigned in terms of ground-state coordinates, the ground surface serves as a "template" for the dynamics on the excited surface. IVR on the excited surface leaves its tracks in the intensities of the vibrational levels of the ground surface. Imagine detuning from a vibrational absorption feature. The lines that disappear first received the energy last, the lines that disappear next received the energy somewhat earlier, etc.[10] By sequentially detuning and monitoring the intensities in these lines one may reconstruct the pathway for energy transfer from benzene ring to alkyl tail.

Acknowledgment. D.J.T. expresses his appreciation to the T-12 group at Los Alamos for their hospitality and to Nelson deLeon in particular. This work was supported by the National Science Foundation and Los Alamos National Laboratories.

Glossary

TF	tense fluorescence
TDF	total dispersed fluorescence
DFS	dispersed fluorescence spectrum
RRS	resonance Raman scattering
RWF	Raman wavefunction

Registry No. Methylbenzene, 108-88-3; *n*-pentylbenzene, 538-68-1; *n*-hexylbenzene, 1077-16-3; *tert*-pentylbenzene, 2049-95-8.

(10) Tannor, D. J. Ph.D. Thesis, University of California, Los Angeles, CA, 1984.